Contribution of T-Type VDCC to TEA-Induced Long-Term Synaptic Modification in Hippocampal CA1 and Dentate Gyrus

Dong Song,[1,4]* Zhuo Wang,[2,3,4] and Theodore W. Berger[1,2,3,4]

[1]*Department of Biomedical Engineering, University of Southern California, Los Angeles, California*
[2]*Department of Biological Sciences, University of Southern California, Los Angeles, California*
[3]*Program in Neuroscience, University of Southern California, Los Angeles, California*
[4]*Center for Neural Engineering, University of Southern California, Los Angeles, California*

ABSTRACT: We have previously reported that exposure to the K^+ channel blocker tetraethylammonium (TEA), 25 mM, induces long-term potentiation (LTP) in CA1, but not in the dentate gyrus (DG), of the rat hippocampal slice. During TEA application, stimulation of excitatory afferents results in a strong depolarizing potential after the fast excitatory postsynaptic potential (EPSP) in CA1, but not in DG. We hypothesized that the differential effect of TEA on long-term synaptic modification in CA1 and DG results from different levels of TEA-elicited depolarization in the two cell types. Additional pharmacological studies showed that blockade of T-type voltage-dependent calcium channels (VDCCs) decreased both the magnitude of LTP and the late, depolarizing potential in CA1. Blockade of L-type VDCCs had no such effect. Using computer models of morphologically reconstructed CA1 pyramidal cells and DG granule cells, we tested our hypothesis by simulating the relative intracellular Ca^{2+} accumulation and membrane potential changes mediated by T-type and L-type VDCCs. Simulation results using pyramidal cell models showed that, with decreased maximum conductance of TEA-sensitive potassium channels, synaptic inputs elicited strong depolarizing potentials similar to those observed with intracellular recording. During this depolarization, VDCCs were opened and resulted in a large intracellular Ca^{2+} accumulation that presumably caused LTP. When T-type VDCCs were blocked, the magnitudes of both the Ca^{2+} accumulation and the late depolarizing potential were decreased substantially. Simulated blockade of L-type VDCCs had only a minor effect. Together, our modeling and experimental studies indicate that T-type VDCCs, rather than L-type VDCCs, are primarily responsible for facilitating the depolarizing potential caused by TEA and for the consequent Ca^{2+} influx. Thus, our findings strongly suggest that the induction of TEA-LTP in CA1 depends primarily on T-type, rather than L-type, VDCCs. Simulation results using modeled granule cells suggests that the failure of TEA to induce LTP in DG is partly due to a low density of T-type VDCCs in granule cell membranes. *Hippocampus 2002;12:689–697.*

KEY WORDS: LTP; LTD; hippocampus; TEA; NMDA receptor; voltage-dependent calcium channel

INTRODUCTION

Long-term potentiation (LTP) can be induced by high-frequency synaptic input (Bliss and Collingridge, 1993) or by pharmacological manipulation, e.g., application of the K^+ channel blocker, tetraethylammonium (TEA) (Aniksztejn and Ben-Ari, 1991; Huang and Malenka, 1993; Hanse and Gustafsson, 1994; Huber et al., 1995; Song et al., 2001). As with high-frequency stimulation (HFS)-induced LTP, TEA-induced LTP (TEA-LTP) depends on elevation of $[Ca^{2+}]_i$ (Huang and Malenka, 1993). In CA1, TEA-LTP has been reported to consist of both N-methyl-D-aspartate glutamate receptor (NMDA)-dependent and voltage-dependent calcium channel (VDCC)-dependent components (Huber et al., 1995; Song et al., 2001). Both L-type (Huang and Malenka, 1993; Huber et al., 1995) and T-type (Song et al., 2001) VDCCs have been reported to contribute to the VDCC-dependent component. In DG, both NMDA-dependent long-term depression (LTD) (Song et al., 2001) and T-type VDCC-dependent LTP have been reported (Coogan et al., 1999).

In a previous investigation (Song et al., 2001), we studied TEA-LTP and TEA-LTD in CA1 and DG, using

Grant sponsor: Office of Naval Research; Grant sponsor: Biomedical Simulations Resource of the National Centers for Research Resources.
*Correspondence to: Dong Song, 403 Hedco Neuroscience Building, University of Southern California, Los Angeles, CA 90089.
E-mail: dsong@usc.edu
Accepted for publication 10 May 2002
DOI 10.1002/hipo.10105

both intracellular and extracellular recording techniques. We observed a correlation between a strong plateau-like depolarizing potential recorded in the presence of TEA and the induction of LTP. LTP was induced in CA1, where the depolarizing potential was strongest, and not in DG, where the depolarizing potential was much weaker. When Ni^{2+} blocked this depolarizing potential significantly, the TEA-LTP observed in CA1 was also largely reduced. In DG, TEA induced NMDA-dependent LTD rather than LTP. The depolarizing potential recorded from granule cells during TEA was small compared with that observed in CA1 pyramidal cells. When $[Ca^{2+}]_o$ was elevated, the depolarizing potential in dentate granule cells was increased and a weak LTP was induced, possibly due to enhanced Ca^{2+} influx through VDCCs.

The contribution of VDCCs to LTP induction may be both direct and indirect. VDCCs mediate calcium influx when opened and can mediate LTP induction directly (Grover and Teyler, 1990). In contrast, any one subtype of VDCC, when activated, also contributes to depolarization of the postsynaptic membrane and will consequently also influence other voltage-dependent sources of Ca^{2+}, such as NMDA receptors and other subtypes of VDCCs. As reported previously by Aradi and Holmes (1999), T-type VDCCs in distal dendrites are responsible for the depolarizing afterpotential (DAP), which is a strong determinant of burst firing.

As stated above, there have been contradictory reports as to the relative contribution of T-type and L-type VDCCs to TEA-LTP. Investigations into the mechanisms of TEA-LTP have been primarily carried out experimentally. Uncontrolled differences in experimental conditions, e.g., the effectiveness of TEA blockade, might be the source of some of the previously reported inconsistencies. Also, selective activation of the different classes of VDCCs involves complex processes that are not easily separable pharmacologically. In this study, we used a computational approach to follow up on our earlier experimental studies of the role of VDCCs in synaptic potentiation. We constructed compartmental models for a CA1 pyramidal cell and a DG granule cell, to study the effects of TEA in a quantitative manner. The relative contributions of different types of VDCCs to both excitatory postsynaptic potential (EPSP) profiles and Ca^{2+} transients were analyzed.

MATERIALS AND METHODS

Experimental Procedures

Hippocampal slices were prepared from adult, male Sprague-Dawley rats (200–250 g). Animals were first anesthetized with 5% halothane and were then decapitated; the hippocampi were rapidly dissected. Both hippocampi were sectioned into blocks while being washed with cold, oxygenated medium, and slices of tissue (400 μm thick) then were cut perpendicular to the longitudinal axis with a vibratome. Slices were incubated with medium consisted of (in mM): 128 NaCl; 2.5 KCl; 1.25 NaH_2PO_4; 26 $NaHCO_3$; 10 glucose; 2 $CaCl_2$; 2.0 $MgSO^4$, aerated with 95% O_2/5% CO_2. Hippocampal slices were maintained at 32°C throughout all experiments. During the experimental session, slices were transferred to the recording chamber and were perfused at flow rates of 4–6 ml/min; the perfusion media was changed to include 1.0 mM $MgSO_4$ and 100 μM picrotoxin (Sigma). Bipolar nichrome stimulating electrodes were placed in the medial perforant path and Schaffer collaterals to permit orthodromic activation of dentate granule cells and CA1 pyramidal cells, respectively. A cut was made between the CA3 and CA1 regions to prevent epileptiform activity in the CA3 region from affecting the recording in CA1. During the application of TEA (25 mM, Sigma), the concentration of NaCl was changed correspondingly to maintain constant osmolarity of the perfusion media. D-APV (50 μM, Tocris), nickel chloride (50 μM, Aldrich), or nifidipine (20 μM, Sigma) was added to the perfusion media when used. Nifidipine was made daily as a 10 mM stock in dimethylsulfoxide (DMSO), stored in the dark, and diluted to 20 μM final concentration in the perfusion medium immediately before application. Application of DMSO (0.05%) alone had no effect on LTP or EPSPs. Field EPSPs of DG granule cells and/or CA1 pyramidal cells were evoked at a frequency of 0.1 Hz by 0.1-ms duration pulses (intensity: 0.04–0.12 mA). Extracellular field EPSPs in CA1 were recorded in stratum radiatum, and the extracellular field EPSPs in DG were recorded in the middle third of the molecular layer. Extracellular recording pipettes were filled with 2 M NaCl (resistance: 1–2 MΩ). Intracellular recording pipettes were filled with 3 M potassium acetate (impedance: 100 MΩ). HFS consisted of four stimulation trains separated by 5-s intervals; each train was composed of 10 pulses at a frequency of 100 Hz and was delivered at the same intensity as that used to evoke baseline responses. All evoked responses were amplified, digitized, and stored using a Pentium PC. Data from different slices were combined by normalizing amplitudes of EPSPs relative to the average response amplitudes measured during the control period. Student's *t*-test was used for statistical comparisons.

Computational Procedures

The NEURON (version 4.3.1) simulation program (Hines and Carnevale, 1997) was implemented on an IBM-compatible PC, running the operating system Windows 2000. The electrophysiological properties of modeled cells were adapted from various sources (Jaffe et al., 1994; Migliore et al., 1995; Aradi and Holmes, 1999). Nine channel types were included in the models: fast sodium channels, three Ca^{2+}-independent potassium channels (K_{DR}, K_A, and K_M), two Ca^{2+}-dependent potassium channels (K_C and K_{AHP}) and three voltage-dependent calcium channels (T-type VDCC, L-type VDCC, and N-type VDCC). All these channels were described by Hodgkin-Huxley-like equations. Ca^{2+} accumulation and extrusion mechanisms also were included to calculate $[Ca^{2+}]_i$. Since very little is known about the spatial distribution and densities of sodium channels and potassium channels in DG granule cells, densities similar to those of CA1 pyramidal cells were used for DG granule cells (Table 1).

The density of VDCCs was based on an estimation from single-channel recordings in adult CA1 pyramidal cells and DG granule

TABLE 1.

Parameters of the Ionic Channels Used to Construct Models of CA1 Pyramidal Cells and DG Granule Cells

Channel density ($pS/\mu m^2$)	CA1 pyramidal cell	DG granule cell
gNa	150	150
gK_{DR}	300	300
gK_A	10	10
gK_M	2	2
gK_{AHP}	4	4
gK_C	6	6
$gVDCC_T$	5	1.5
$gVDCC_N$	20	30
$gVDCC_L$	20	3

DG, dentate gyrus; VDCC, voltage-dependent calcium channel (T, N, L types); g (conductance).

cells (Fisher et al., 1990). In the modeled CA1 pyramidal and DG granule cells, T-N-L channel density ratios of 10:22:13 and 3:30:2 were used. These ratios were then weighted by the single-channel conductance (8-pS, 14-pS, 25-pS for T-type, N-type, L-type VDCC, respectively) to obtain the maximum conductance ratios (1:4:4 in the CA1 pyramidal model and 1:20:2 in the DG granule model). All channels were assumed to be evenly distributed throughout the cells.

The morphology for the CA1 pyramidal cell model was adapted from a previous publication by Migliore et al. (1995). The morphology for the DG granule cell model was modified from Claiborne et al. (1990). Synaptic input was modeled as an α function with $\alpha^{-1} = 3$ ms. For simplicity, NMDA channels were not included in the models because the essential question addressed concerned the relative contribution of T-type and L-type VDCCs to TEA-LTP.

RESULTS

Extracellular and Intracellular Recording

Differential effects of TEA on synaptic modification and EPSP profile in CA1 and DG

Field potentials generated within CA1 and DG were recorded simultaneously from the same hippocampal slices. As we previously reported, TEA induced robust LTP in CA1 only (Fig. 1C; n = 9), while HFS induced robust LTP in both CA1 and DG (Fig. 1A,B). Instead of LTP, a weak but significant LTD was induced in DG 30–60 min after TEA application (Fig. 1D; n = 14). Another differential effect of TEA, which we hypothesized to be the cause of the above differential effect on the synaptic modification, was found in the EPSP responses to single pulse stimulation during TEA application. In CA1, there was a large, late depolarizing component after the fast EPSP, which could last >100 ms (Fig. 1E,b). In DG, only a weak late component of much shorter duration was observed after the EPSP (Fig. 1F,b).

Marked differences between intracellular recordings from CA1 and dentate also were observed. In CA1 pyramidal cells, bursts of action potentials and a strong depolarizing potential were elicited in the presence of TEA (Fig. 1G,b). In DG granule cells, there was neither a burst of action potentials nor a depolarizing potential, although the single action potential was significantly broadened, as it was for CA1 pyramidal cells (Fig. 1H,b). Consistent with the field potential results, TEA induced LTP intracellular EPSPs in CA1 (n = 3; data not shown), but LTD in DG measured 60 min after TEA application (n = 4; data not shown).

Effect of channel blockers on TEA-induced synaptic modification and EPSP responses during TEA application

To determine the contribution of NMDA receptors and VDCCs to the induction of TEA-induced LTP/LTD, D-APV (50 μM), nifidipine (20 μM) and Ni^{2+} (50 μM) were applied to the bath to block NMDA receptors, L-type VDCCs and T-type VDCCs, respectively. D-APV partially blocked the TEA-LTP in CA1 (Fig. 2A; n = 5) and completely blocked the TEA-LTD in DG (Fig. 2B; n = 5). The L-type VDCC blocker, nifidipine, did not have a significant effect on either TEA-LTP in CA1 (Fig. 2A; n = 5) or TEA-LTD in DG (Fig. 2B; n = 4).

At the concentration used in our study, Ni^{2+}, the T-type VDCC blocker, partially blocked TEA-LTP in CA1 without significantly altering the amplitude of baseline EPSPs (Fig. 2A; n = 5). The combined application of D-APV and Ni^{2+} strongly suppressed TEA-LTP in CA1 (Fig. 2A; n = 6). Ni^{2+} did not block TEA-LTD in DG (Fig. 2B; n = 6). The correlation of LTP induction with the late component depolarization was observed again: Ni^{2+} significantly decreased the late component of EPSPs in CA1. The combined application of D-APV and Ni^{2+} decreased the late component even more markedly (Fig. 2C).

Although TEA induced LTD in DG under normal conditions, when the extracellular Ca^{2+} concentration was increased (4 mM), a weak LTP was induced (Fig. 2B; n = 5). Interestingly, the late component was also increased in the presence of high extracellular Ca^{2+} (Fig. 2D). This result supports our hypothesis that LTP induction depends on the depolarizing potential after the fast EPSP. When Ni^{2+} was added to the bath, the effects of high Ca^{2+} concentration were reversed (Fig. 2B,D; n = 4). This result showed that LTP induction and late component in DG also depend on the activity of T-type VDCCs.

Computer Simulations

EPSP profiles in the presence of TEA in CA1

The maximum conductance of five types of K^+ channels (gK_{DR}, gK_C, gK_A, gK_M, and gK_{AHP}) was decreased from original values,

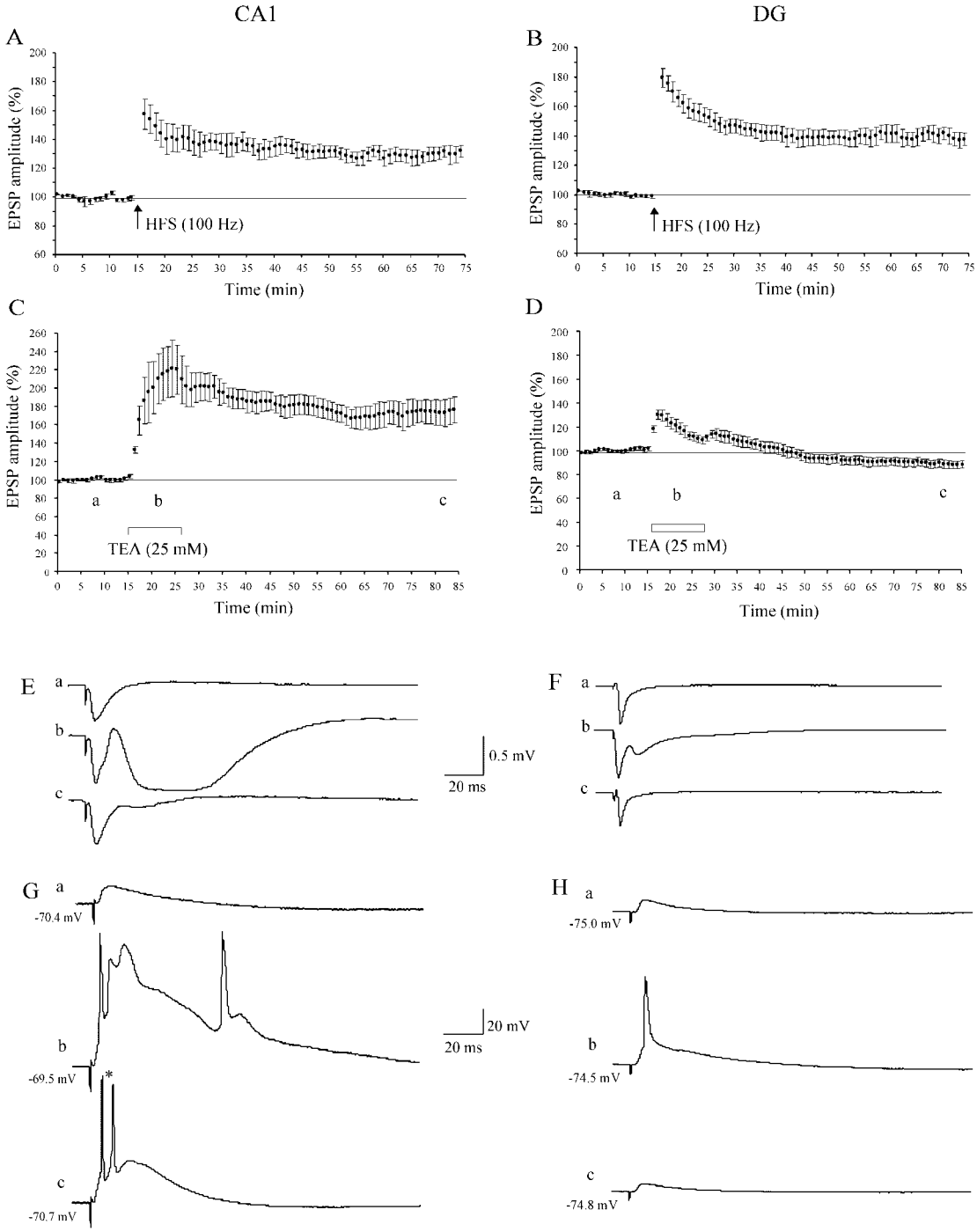

FIGURE 1. High-frequency stimulation (HFS) and tetraethylammonium (TEA)-induced synaptic modification in CA1 and dentate gyrus (DG). A: HFS (100 Hz) induced long-term potentiation (LTP) in CA1. B: HFS (100 Hz) induced LTP in DG. C: TEA (25 mM) induced LTP in CA1. D: TEA (25 mM) failed to induce LTP in DG. A 10-min bath application of 25 mM TEA resulted in a weak but significant LTD in DG. Graphs in C–H: a, before TEA application; b, during TEA application; c, 60 min after washout of TEA. E: Representative field excitatory postsynaptic potentials (EPSPs) recorded from stratum radiatum in CA1. Note that TEA resulted in a large, depolarizing potential in addition to enhancing the fast component of EPSPs. F: Representative field EPSPs recorded from the middle third of the molecular layer in DG. G: Representative intracellular EPSPs recorded from a pyramidal cell in CA1. Note that membrane potentials were barely changed during TEA application in both pyramidal and granule cells. A strong depolarizing potential was present in CA1 pyramidal cell (*), but not in DG granule cell. H: Representative intracellular EPSPs recorded from a granule cell in DG.

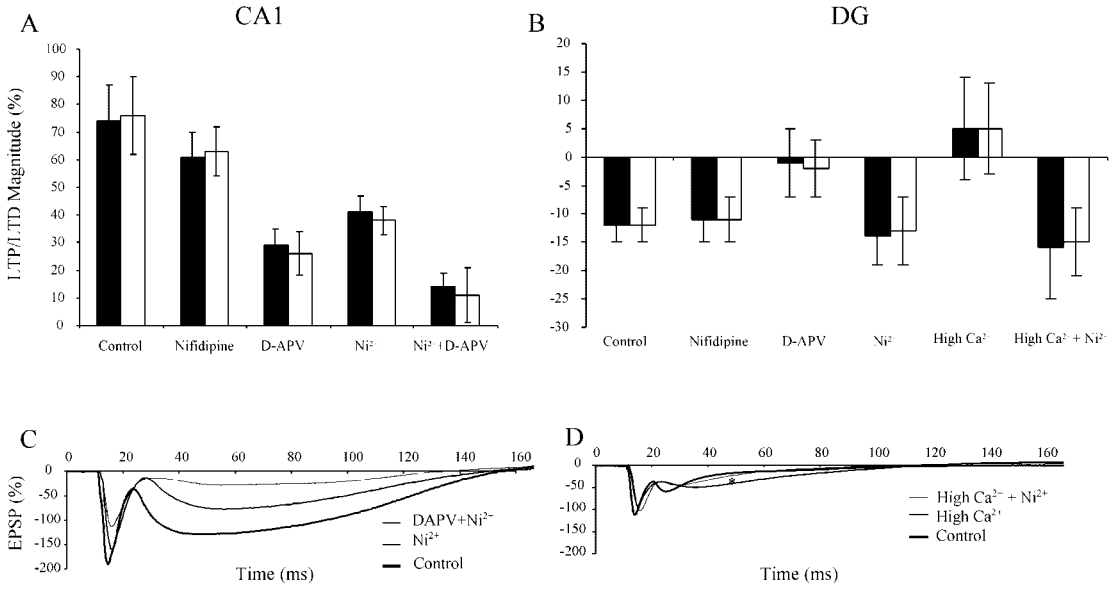

FIGURE 2. Tetraethylammonium-induced long-term potentiation (TEA-LTP) in CA1 is both NMDA receptor- and T-type voltage-dependent calcium channel (VDCC)-dependent, while TEA-LTD in dentate gyrus (DG) is only NMDA-dependent. The TEA-elicited depolarizing potential in DG is increased by raising extracellular Ca^{2+} concentration, resulting in the reversal of TEA-LTD. The depolarizing potential in both CA1 and DG is mediated chiefly by T-type VDCC. In A and B, black bar. peak amplitude of excitatory postsynaptic potential (EPSP) measured 60 min after TEA application; white bar. maximum slope of EPSP measured 60 min after TEA application. A: In CA1, L-type VDCC blocker, nifidipne (20 μM) did not block the TEA-LTP. D-APV (50 μM) and Ni^{2+} (50 μM) partially blocked the TEA-LTP. A combined application of Ni^{2+} (50 μM) and D-APV (50 μM) strongly blocked the TEA-LTP. B: in DG, neither nifidipne (20 μM) nor Ni^{2+} (50 μM) blocked the TEA-LTD. D-APV (50 μM) completely blocked the TEA-LTD. In medium with doubled Ca^{2+} concentration (4 mM), TEA induced weak LTP in DG. This LTP was reversed by Ni^{2+} (50 μM). C: EPSP profiles during the TEA application in CA1. In both C and D, EPSPs were first averaged and normalized within single slices, and then averaged across different slices. Note that the large, late, depolarizing potential was partially blocked by Ni^{2+} (50 μM) application (medium line) and strongly blocked by the combined application (thin line) of Ni^{2+} (50 μM) and D-APV (50 μM) compared with the late component under control condition (thick line). D: EPSP profiles during the TEA application in DG. Note that in 4 mM Ca^{2+} medium (medium line), the depolarizing potential increased significantly (*) compared with that in 2 mM Ca^{2+} medium (thick line). This increase was blocked by Ni^{2+} (50 μM) application (thin line).

shown in Table 1, to simulate the effect of TEA on CA1 pyramidal cells. According to previous reports (Storm, 1990), K_{DR} and K_C are sensitive to TEA, while K_A, K_M, and K_{AHP} are less sensitive to TEA. In our simulations, gK_{DR} and gK_C were decreased to 5–70% of their original values and gK_A, gK_M, and gK_{AHP} were decreased to 20–90% of their original values to reflect the different degrees of blockade by TEA. By manipulating the maximum conductance of these K^+ channels, several forms of intracellularly recorded CA1 EPSP profiles during TEA application could be replicated (Fig. 3). When high blockade of K^+ channels was simulated (gK_{DR}, 5%; gK_C, 5%; gK_A, 20%; gK_M, 20%; gK_{AHP}, 20%), there was a large, persistent depolarizing potential merged with an action potential (Fig. 3A). Moderate blockade of K^+ channels (gK_{DR}, 30%; gK_C, 10%; gK_A, 60%; gK_M, 60%; gK_{AHP}, 60%), was associated with EPSP profiles similar to those observed for CA1 pyramidal neurons during TEA application (Fig. 3B). When low blockade of K^+ channels was simulated (gK_{DR}, 70%; gK_C, 70%; gK_A, 70%; gK_M, 70%; gK_{AHP}, 70%), the result was bursts of action potentials without the plateau-like depolarizing potential (Fig. 3C). This kind of waveform was similar to the EPSP profiles recorded intracellularly from CA1 pyramidal cells during both the early phase of TEA application and during the washout of TEA.

T-type VDCCs facilitate the elicitation of the depolarizing potential in CA1

Without TEA application (original maximum conductance of K^+ channels), simulated single-pulse activation of synaptic input elicited EPSPs or single action potentials, depending on the input magnitude, in modeled CA1 pyramidal cells. An example simulated single action potential followed by a DAP is shown in Figure 4A,b. Single action potentials caused a small $[Ca^{2+}]_i$ increase in both the dendritic and somatic regions of the cell (Fig. 4A,a). The $[Ca^{2+}]_i$ increase was much higher in the dendrite than in the soma because of the larger surface volume ratio in dendrite (Fig. 4A,a). This low level of $[Ca^{2+}]_i$ increase with low input frequencies does not induce long-term synaptic modification experimentally. In our experimental recordings, the stimulation intensity was controlled so as to remain subthreshold for action potential generation, so the Ca^{2+} influx into the neuron was even lower than the simulation results in the present study.

When TEA application was simulated with the parameters described above, all three subtypes of VDCCs opened during action potential generation and the plateau-like depolarizing potential, resulting in a dramatic increase in $[Ca^{2+}]_i$ in both dendritic and

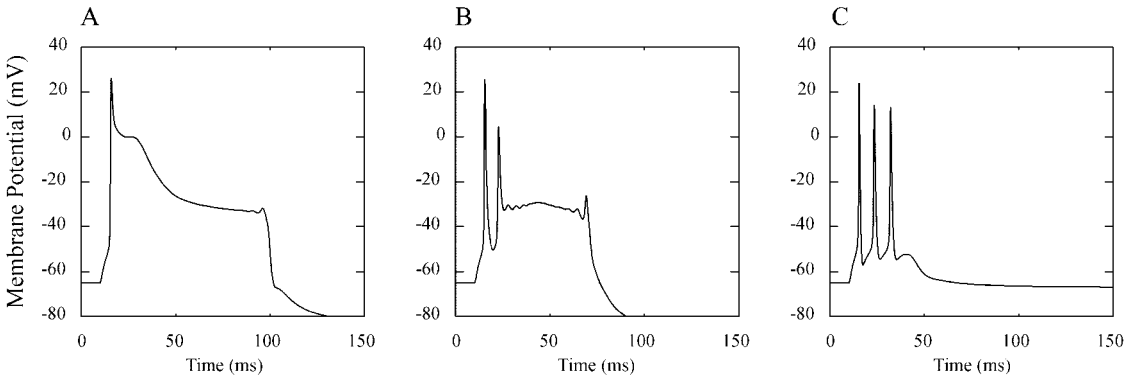

FIGURE 3. Effect of tetraethylammonium (TEA) on the excitatory postsynaptic potential (EPSP) profiles was simulated by decreasing the maximum conductance of K^+ channels. A: When the maximum conductance of K^+ channels was extremely low, there was a strong depolarizing potential merged with the action potential. B: When the maximum conductance of K^+ channels was low, there was a plateau-like depolarizing potential after the first action potential. C: When the maximum conductance of K^+ channels was close to the normal value, there was burst of action potentials.

somatic compartments of the modeled CA1 pyramidal cell (Fig. 4B,a). The $[Ca^{2+}]_i$ in the dendrite reached 170 nM, which was more than three times resting $[Ca^{2+}]_i$.

When the maximum conductance of T-type VDCCs was set to zero to simulate the blockade by Ni^{2+}, TEA failed to cause a second action potential or the plateau-like depolarizing potential (Fig. 4C,b). L-type and N-type VDCC conductance was greatly reduced because of the low level of depolarization, resulting in a small $[Ca^{2+}]_i$ increase (Fig. 4C,a). The marked suppression by Ni^{2+} of membrane depolarization and calcium influx was simulated for a broad range of maximum K^+ channel conductance (i.e., simulated degree of K^+ channel blockade) (Fig. 5). When gK_{DR} was decreased to 30–70% of its original value, Ni^{2+} suppressed the EPSP profiles to single action potentials, and the $[Ca^{2+}]_i$ increase caused by TEA was decreased by 75–85%. (Note that in these simulations, gK_C, gK_A, gK_M, and gK_{AHP} also were decreased according to the ratios given in the Methods section). When gK_{DR} was decreased to less than 30%, modeled CA1 neurons exhibited bursts of action potentials despite the Ni^{2+} blockade of T-type VDCCs. Ca^{2+} influx was predominantly via high-threshold N-type VDCCs. The decrease in $[Ca^{2+}]_i$ caused by Ni^{2+} was less dramatic than in the previous case, but still significant (30–40%). The blockade of L-type VDCCs did not significantly affect the EPSP profiles (Fig. 4D,b) or $[Ca^{2+}]_i$ accumulation (Figs. 4D,a and 5).

DG granule cell simulation results

In our models, we assumed that the densities of VDCCs are the only differences in electrophysiological properties between the CA1 pyramidal cell and the DG granule cell. Our result showed that TEA (gK_{DR}, 10%; gK_C, 10%; gK_A, 60%; gK_M, 60%; gK_{AHP}, 60%) failed to elicit bursts of action potentials and plateau-like depolarizing potentials in DG granule cell models (Fig. 6B). There were two mechanisms, in combination, responsible for this differential effect of TEA on the dynamics of the two cell models. First, the density of T-type VDCCs in the DG granule cell model was much lower than that in the CA1 pyramidal cell model (1.5 pS/μm^2 vs 5.0 pS/μm^2 for DG and CA1, respectively). Increasing the maximum conductance of T-type VDCCs alone was able to reverse the granule cell model to a bursting state. Second, even when the same densities of VDCCs were assigned to the two cell models (i.e., the only difference between the two models was the morphology), the DG granule cell model was still more resistant to TEA than the CA1 pyramidal cell model (data not shown). This result suggested that morphology also was a factor responsible for the high resistance to TEA-elicited late depolarization in DG granule cells.

DISCUSSION

We previously reported a differential effect of TEA on long-term synaptic modification in the CA1 and DG regions of hippocampus: TEA induces robust LTP in CA1 but weak LTD in DG. We also found that in CA1, the induction of TEA-LTP is always accompanied by a strong depolarizing potential during TEA application. In DG, there is only a weak depolarizing potential (Song et al., 2001). Previous studies have showed that TEA-induced LTP, like HFS-induced LTP, depends on an increase in postsynaptic $[Ca^{2+}]_i$ (Huang and Malenka, 1993). In contrast to HFS LTP, in which the main contributors of the Ca^{2+} influx are NMDA-receptor channels, the Ca^{2+} influx that induces TEA-LTP is mediated primarily by VDCCs (Grover and Teyler, 1990; Aniksztejn and Ben-Ari, 1991; Huang and Malenka, 1993; Hanse and Gustafsson, 1994; Huber et al., 1995). TEA blocks K^+ channels and enhances depolarization, VDCCs are opened by this depolarization, which results in the $[Ca^{2+}]_i$ increase required to induce LTP. Based on this knowledge and the differential effects of TEA in CA1 and DG, we hypothesized that the strength of depolarizing potential might determine the probability of LTP induction. Namely, when TEA caused strong depolarization, there

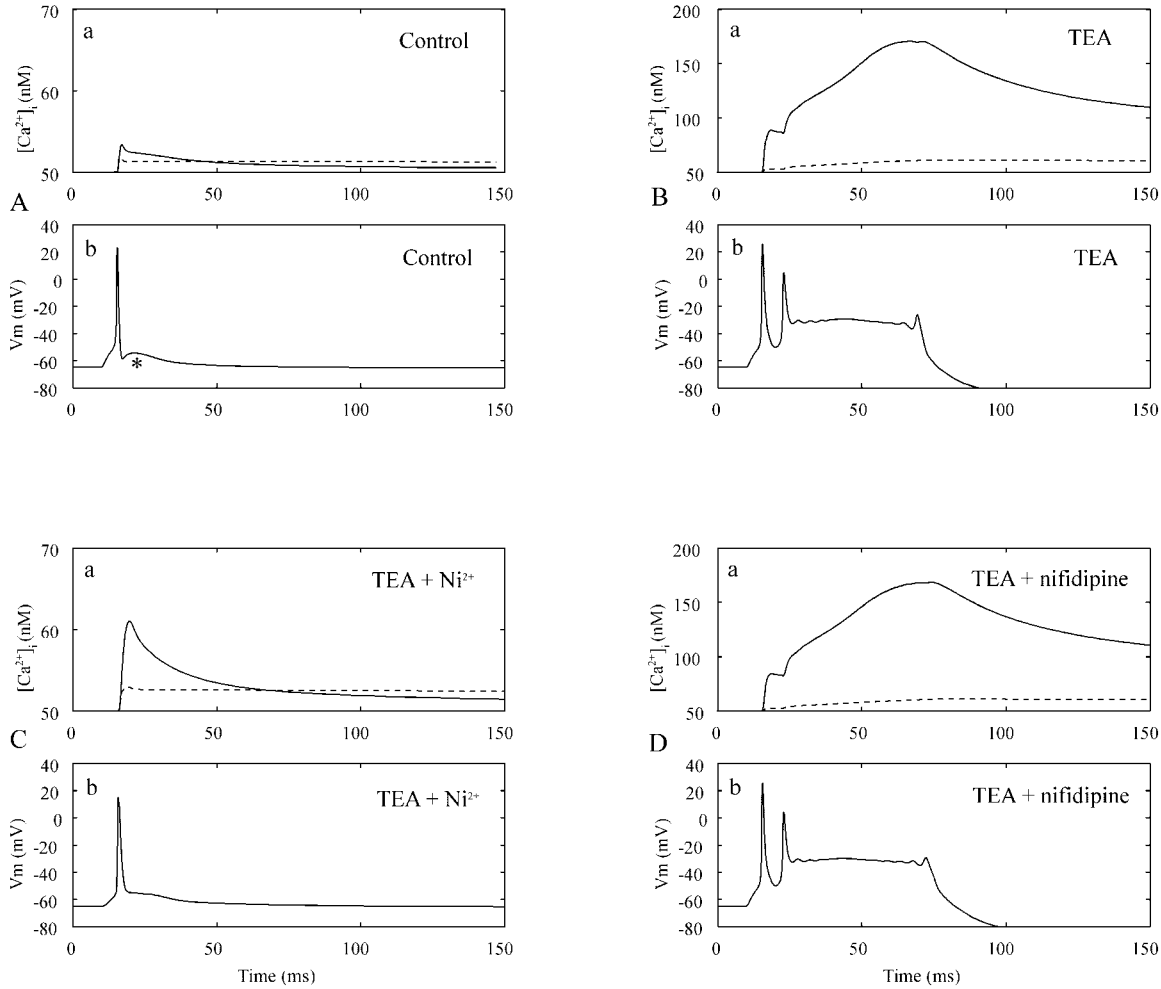

FIGURE 4. T-type voltage-dependent calcium channel (VDCC) facilitated the elicitation of depolarizing potentials. A: Under normal conditions, the synaptic input elicited single action potential and a small $[Ca^{2+}]_i$ increase. Note that there was a DAP after the action potential (*). A–D: (a) Dashed line, $[Ca^{2+}]_i$ in soma; solid line, $[Ca^{2+}]_i$ in dendrite; (b) solid line, membrane potential in soma. B: When the maximum conductance of K^+ channels was decreased, there were burst of action potentials and plateau-like depolarizing potential. $[Ca^{2+}]_i$ in both soma and dendrite largely increased. C: When T-type VDCC was blocked, tetraethylammonium (TEA) failed to cause the depolarizing potential. The $[Ca^{2+}]_i$ increase was small compared with the TEA case in B. D: When L-type VDCC was blocked, there was no significant change in excitatory postsynaptic potential (EPSP) profile or $[Ca^{2+}]_i$ compared with the TEA case in B.

would be more VDCCs open and allowed high $[Ca^{2+}]_i$ increase that resulted in LTP; when TEA caused weak depolarization, fewer VDCCs were open and resulted in LTD or weaker LTP.

The major finding of this series of studies was that T-type VDCCs are critical for the depolarizing potential and the subsequent induction of TEA-LTP induction. In CA1 pyramidal cells, Ni^{2+}, the T-type VDCC blocker, suppressed the depolarizing potentials during TEA application and partially blocked LTP. This result provided another example of the positive correlation between the two phenomena and suggests that T-type VDCCs are a major mediator of the induction of TEA-LTP. To test this hypotheses, we constructed compartmental hippocampal neuron models incorporating real morphology and nine major ionic channels. In these models, we reduced the conductance of various K^+ channels to simulate the pharmacological effects of TEA and calculated the membrane potential and intradendritic Ca^{2+} concentration. The latter was assumed to be the determining factor for LTP induction. Our modeling results showed that for a broad range of simulated K^+ channel blockade, T-type VDCCs were needed to elicit bursts of action potentials and the plateau-like depolarizing potential similar to that observed experimentally during intracellular recording. In other words, decreased T-type VDCC conductance results in weaker depolarization and lower $[Ca^{2+}]_i$ increases. T-type VDCCs are not only a major source for Ca^{2+} influx, but also facilitate the strong depolarizing potential caused by TEA which, in turn, opens other types of VDCCs. In contrast, when L-type VDCC blockade was simulated, there were only moderate changes in stimulation-induced EPSP profiles, and Ca^{2+} influx via other types of VDCCs was still large enough to substantially raise $[Ca^{2+}]_i$.

In our previous experiments with DG granule cells, we found that TEA induced LTD instead of LTP, and that the depolarizing

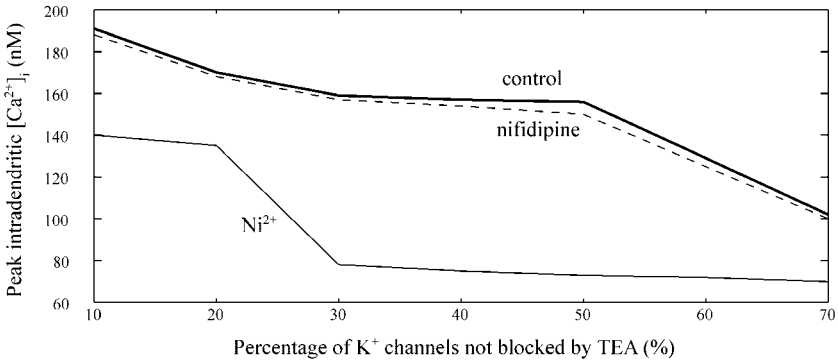

FIGURE 5. The contributions of T-type and L-type voltage-dependent calcium channels (VDCCs) to $[Ca^{2+}]_i$ under different levels of K^+ channel blockade. The K^+ channels were blocked from 10% to 70%. Top thick line. peak $[Ca^{2+}]_i$ in dendrite; Middle dashed line. peak $[Ca^{2+}]_i$ in dendrite without L-type VDCC; bottom thin line. peak $[Ca^{2+}]_i$ in dendrite without T-type VDCC.

potentials during TEA application were much smaller compared with those observed in CA1 pyramidal cells. If TEA-LTP induction really depends on the depolarizing potential, it should be possible to reverse the TEA-LTD to TEA-LTP in DG if the TEA-induced depolarizing potential were increased. We tested this hypothesis by increasing Ca^{2+} concentration in the perfusion bath. Our results showed that high $[Ca^{2+}]_o$ increased the magnitude of the depolarizing potential significantly and induced a weak LTP. As in CA1, both the depolarizing potential and the TEA-LTP were blocked by Ni^{2+}. However, the magnitude of the late depolarizing component and the subsequent LTP were much smaller than that observed in CA1. These results, combined with the simulation data from modeled DG granule cells, suggests a low density of T-type VDCCs in DG granule cells. This is consistent with an earlier report by Fisher et al. (1990). In their study, the density of T-type, L-type, and N-type VDCCs was estimated by calculating the relative frequency of observing the three channel types in cell-attached patches. The results reported by Fisher and colleagues showed that the density of T-type VDCCs was much lower in DG granule cells than in CA1 pyramidal cells.

Coogan et al. (1999) reported that TEA induced a T-type VDCC-dependent LTP in young rat hippocampal DG granule cells, instead of the LTD that we have observed experimentally. This apparent discrepancy might result from the differences in the density of T-type VDCCs in young versus mature rat hippocampus. Several studies have shown that T-type VDCCs are predominant in immature DG granule cells, while the presence of T-type current in adult DG granule cells is still controversial (Fisher et al., 1990; Kohr and Mody, 1991; Zhang et al., 1993). This decreased prominence of the DAP and LTP induction in adulthood is very likely caused by the down-regulation of T-type VDCCs during development.

In contrast to an earlier report (Huang and Malenka, 1993), our experimental results showed that T-type VDCCs, instead of L-type VDCCs, play an important role in determining the induction of TEA-LTP in the CA1 region. Our experimental findings are supported by our simulation results showing that L-type VDCCs have no significant effect on either EPSP profiles or Ca^{2+} accumulation. Consistent with an earlier study (Huber et al., 1995), we found experimentally that NMDA receptor-channels also contribute to TEA-LTP in CA1. During TEA application, CA1 pyramidal cells exhibited strong depolarizations and bursts of action potentials. Considering the voltage-dependent blockade of the NMDA receptor channel, it is possible that these depolarizing

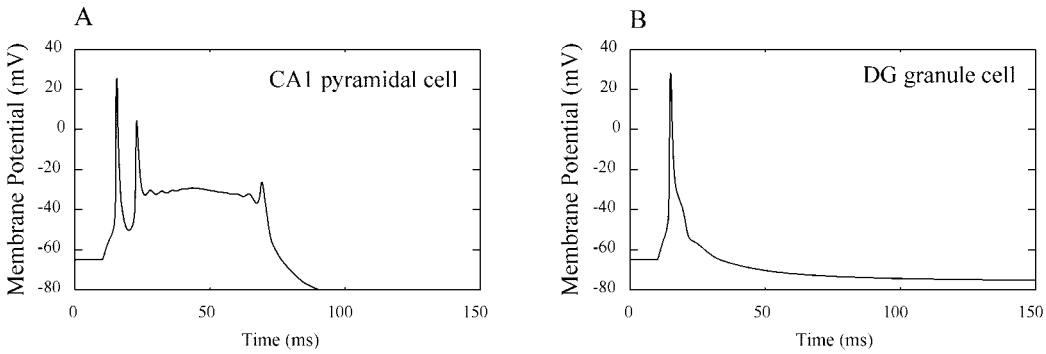

FIGURE 6. Differential effects of tetraethylammonium (TEA) on excitatory postsynaptic potential (EPSP) profiles in CA1 pyramidal cell and dentate gyrus (DG) granule cell. A: In CA1, TEA elicited burst of action potentials and strong depolarizing potential. B: In DG, there was only single action potential broadened by TEA.

events induced an NMDA-dependent LTP similar to HFS-induced LTP. In DG granule cells, the enhancement of depolarization by TEA was much weaker compared with that in CA1 and, as a consequence, the Ca^{2+} influx was much reduced. It has been established that low levels of Ca^{2+} influx are associated with LTD, as we observed for the DG (Xie et al., 1992).

Our experiments and simulations were carried out on CA1 pyramidal cells and DG granule cells; studies of CA3 pyramidal cell were not included in our analyses. However, the density of T-type VDCCs in CA3 is the highest among these three cell types (Fisher et al., 1990). The importance of T-type VDCCs in LTP induction and burst firing found in this study suggest that activation of T-type VDCCs might serve as a principal mechanism in regulating the capacity for plasticity and bursting property of neurons and synapses in the three nodes of the trisynaptic circuit of hippocampus.

REFERENCES

Aniksztejn L, Ben-Ari Y. 1991. Novel form of long-term potentiation produced by a K^+ channel blocker in the hippocampus. Nature 349: 67–69.

Aradi I, Holmes WR. 1999. Role of multiple calcium and calcium-dependent conductances in regulation of hippocampal dentate granule cell excitability. J Comp Neurosci 6:215–235.

Bliss TV, Collingridge GL. 1993. A synaptic model of memory: long-term potentiation in the hippocampus. Nature 361:31–39.

Claiborne BJ, Amaral DG, Cowan WM. 1990. Quantitative, three-dimensional analysis of granule cell dendrites in the rat dentate gyrus. J Comp Neurol 302:206–219.

Coogan AN, O'Leary DM, O'Connor JJ. 1999. P42/44 MAP kinase inhibitor PD98059 attenuates multiple forms of synaptic plasticity in rat dentate gyrus in vitro. J Neurophysiol 81:103–110.

Fisher RE, Gray R, Johnston D. 1990. Properties and distribution of single voltage-gated calcium channels in adult hippocampal neurons. J Neurophysiol 64:91–104.

Grover LM, Teyler TJ. 1990. Two components of long-term potentiation induced by different patterns of afferent activation. Nature 347:477–479.

Hanse E, Gustafsson B. 1994. TEA elicits two distinct potentiations of synaptic transmission in the CA1 region of the hippocampal slice. J Neurosci 14:5028–5034.

Hines ML, Carnevale NT. 1997. The NEURON simulation environment. Neural Comput 9:1179–1209.

Huang YY, Malenka RC. 1993. Examination of TEA-induced synaptic enhancement in area CA1 of the hippocampus: the role of voltage-dependent Ca^{2+} channels in the induction of LTP. J Neurosci 13: 568–576.

Huber KM, Mauk MD, Kelly PT. 1995. Distinct LTP induction mechanisms: contribution of NMDA receptors and voltage-dependent calcium channels. J Neurophysiol 73:270–279.

Jaffe DB, Ross WN, Lisman JE, Lasser-Ross N, Miyakawa H, Johnston D. 1994. A model for dendritic Ca^{2+} accumulation in hippocampal pyramidal neurons based on fluorescence imaging measurements. J Neurophysiol 71:1065–1077.

Kohr G, Mody I. 1991. Endogenous intracellular calcium buffering and the activation/inactivation of HVA calcium currents in rat dentate gyrus granule cells. J Gen Physiol 98:941–967.

Migliore M, Cook EP, Jaffe DB, Turner DA, Johnston D. 1995. Computer simulations of morphologically reconstructed CA3 hippocampal neurons. J Neurophysiol 73:1157–1168.

Song D, Xie X, Wang Z, Berger TW. 2001. Differential effect of TEA on long-term synaptic modification in hippocampal CA1 and dentate gyrus in vitro. Neurobiol Learn Mem 76:375–387.

Storm JF. 1990. Potassium currents in hippocampal pyramidal cells. Prog Brain Res 83:161–187.

Xie X, Berger TW, Barrionuevo G. 1992. Isolated NMDA receptor-mediated synaptic responses express both LTP and LTD. J Neurophysiol 67:1009–1013.

Zhang L, Valiante TA, Carlen PL. 1993. Contribution of the low-threshold T-type calcium current in generating the post-spike depolarizing afterpotential in dentate granule neurons of immature rats. J Neurophysiol 70:223–231.